J Nanopart Res (2012) 14:740
DOI 10.1007/s11051-012-0740-9

RESEARCH PAPER

Sedimentation of Fe_3O_4 nanosized magnetic particles in water solution enhanced in a gradient magnetic field

I. Medvedeva · M. Uimin · A. Yermakov · A. Mysik · I. Byzov · T. Nabokova · V. Gaviko · N. Shchegoleva · S. Zhakov · V. Tsurin · O. Linnikov · I. Rodina · V. Platonov · V. Osipov

Received: 8 February 2011 / Accepted: 14 January 2012 / Published online: 9 February 2012

Abstract The sedimentation dynamic of magnetite (Fe_3O_4) nanoparticles in water was investigated, both in the presence of a vertical gradient magnetic field and in the gravitational field only. The nanopowders (four samples with average particle diameter ranging from 16 to 84 nm) were prepared by a gas-condensation synthesis method. The sedimentation was monitored by measuring the light transmission coefficient k of the suspension as a function of time. The sedimentation process is of rather complex character for both the large and the small particles. Specifically, the light transmission reflects the different stages of the particle aggregation. Magnetite nanoparticles tend to aggregate into micron-sized aggregates which sediment rather rapidly in high concentrated suspensions (for example 5 g/L), even in the absence of a magnetic field. Gradient magnetic fields (for example $H = 6$ kOe, $dH/dz = 1.6$ kOe/cm) help to increase the sedimentation rate tremendously and reduce the total sedimentation time from several days up to several minutes—here for an average particle size of 16 nm. An effective removal of heavy metal pollutants (Cr, Cu, etc.) from water can be achieved using the optimal combination of the magnetite particle size, particle concentration in water suspension, and magnetic field strength and gradient.

Keywords Magnetite · Nanoparticles · Water · Aggregation · Sedimentation · Gradient magnetic field

I. Medvedeva (✉) · M. Uimin · A. Yermakov · A. Mysik · I. Byzov · T. Nabokova · V. Gaviko · N. Shchegoleva · S. Zhakov · V. Tsurin
Institute of Metal Physics, Ural Branch of the Russian Academy of Sciences, S. Kovalevskaya 18, Yekaterinburg, Russia 620990
e-mail: ivmed@imp.uran.ru

O. Linnikov · I. Rodina
Institute of Solid State Chemistry, Ural Branch of the Russian Academy of Sciences, Pervomayskaya 91, Yekaterinburg, Russia 620990

V. Platonov · V. Osipov
Institute of Electrophysics, Ural Branch of the Russian Academy of Sciences, Amundsena 106, Yekaterinburg, Russia 620016

Introduction

Stock waters from industrial plants in particular those from machinery and metallurgical industry contain a big amount of heavy metal cations, such as iron, copper, nickel, zinc, chromium etc. In the case of insufficient water cleaning this leads to a significant pollution of surface and ground waters. Specifically, the presence of hexavalent chromium is harmful in natural waters due to its high toxicity. The cleaning of stock and natural waters from heavy metal cations is a problem of primary importance both for a clean environment and for the public health situation.

Nanopowder sorbents are promising materials for water purification techniques because of the high specific surface area to volume ratio (e.g., Zhang

2003; Tiwari et al. 2008). However, a very small particle size makes the process of the sorbent separation from the solution by conventional methods (precipitation, filtration, etc.) rather difficult. This problem can be solved by injecting magnetic nanoparticles followed by a removal of the powder from solution in a gradient magnetic field. The primary candidates for magnetic sorbents are iron and its oxides. The elemental iron particles have the large value of magnetization ($\sigma_{S\ 300K} = 218$ emu/g) and as usual they are oxidized at the surface. Therefore, they present a multiphased system both structurally and magnetically which requires to be covered by some shell to avoid a further oxidation in water. Among the iron oxides the ferrimagnetic magnetite Fe_3O_4 has rather substantial magnetization (for the bulk magnetite $\sigma_{S\ 300K} = 92$ emu/g), which makes it another attractive candidate for the magnetic separation in the course of water cleaning.

Usually, the water cleaning by adsorption method includes two simultaneously ongoing processes—the sorption of the pollutants by the sorbent particles and the particle aggregation in water solution. While the particle aggregation can decrease the effective sorption, it favors a better sedimentation which can be used for the subsequent separation of the sorbent from the water solution. The iron oxides nanoparticles surface properties which are important for a sorption, aggregation, and sedimentation processes are dependent on the preparation route (Tartaj et al. 2003). Tiny changes in the local structure of the outer surface of the particles core like oxygen deficiency, local ionic disorder etc. can be strongly modified by the preparation details and thus change the cleaning ability of the magnetic sorbent. Besides, particles coating with mineral and organic substances as well as pH variations are effective means to tune aggregation and sorption properties (Zhong et al. 2006; Liu et al. 2008; Illes and Tombacz 2006; Yuan et al. 2009).

During the last years intensive studies were devoted to the application of magnetic iron oxides nanoparticles for water cleaning from heavy metals (Hu et al. 2004, 2005; Yantasee et al. 2007; Tuutijärvi et al. 2009 and refs. herein). In the majority of the studies the particles were produced by a chemical precipitation method.

The gas-condensation synthesis and the laser evaporation method which allow to make single phase nanoparticles with dimensions from several to hundreds of nanometers (Kortov et al. 2008) are less extensively explored. While the sorption process by nanopowders is being intensively studied the sedimentation of nanopowders in water still requires more attention. In particular, the sedimentation of magnetic nanopowders in a gradient magnetic field presents a special interest for future applications. Therefore, in this study we studied the sedimentation of magnetite nanoparticles prepared by a gas-condensation method both in gravity field only and in a gradient magnetic field.

The samples preparation and characterization

The powder samples of Fe_3O_4 were prepared by gas-condensation method (Kortov et al. 2008). A strongly overheated drop of molten iron was evaporated in a buffer Ar gas media containing some percent of the oxygen. A variation of the partial argon pressure and of the speed of its flowing near the evaporation zone allowed to change the particle sizes. Four types of nanopowders with different average particle sizes were prepared by this method and studied (Table 1).

The phase composition and the crystal structure were examined by X-ray using DRON diffractometer at Cu-K_α radiation. The X-ray analysis showed that the powder samples had a distorted cubic structure with a small tetragonal or orthorhombic distortion and the lattice parameters were close to that of the bulk

Table 1 Properties of Fe_3O_4 nanoparticles for sedimentation study

Sample	Crystal structure and phase composition	Average particle diameter (TEM and XRD) d_{av} (nm)	Specific surface (BET) (m^2/g)	Saturation magnetization (300 K) (emu/g)
N1	100% Defect tetragonal	16	44	81
N2	Defect tetragonal 4% α-Fe	54	21	70
N3	Orthorhombic, 5% α-Fe	18	70	74
N4	Orthorhombic, 5% α-Fe	84	14	81

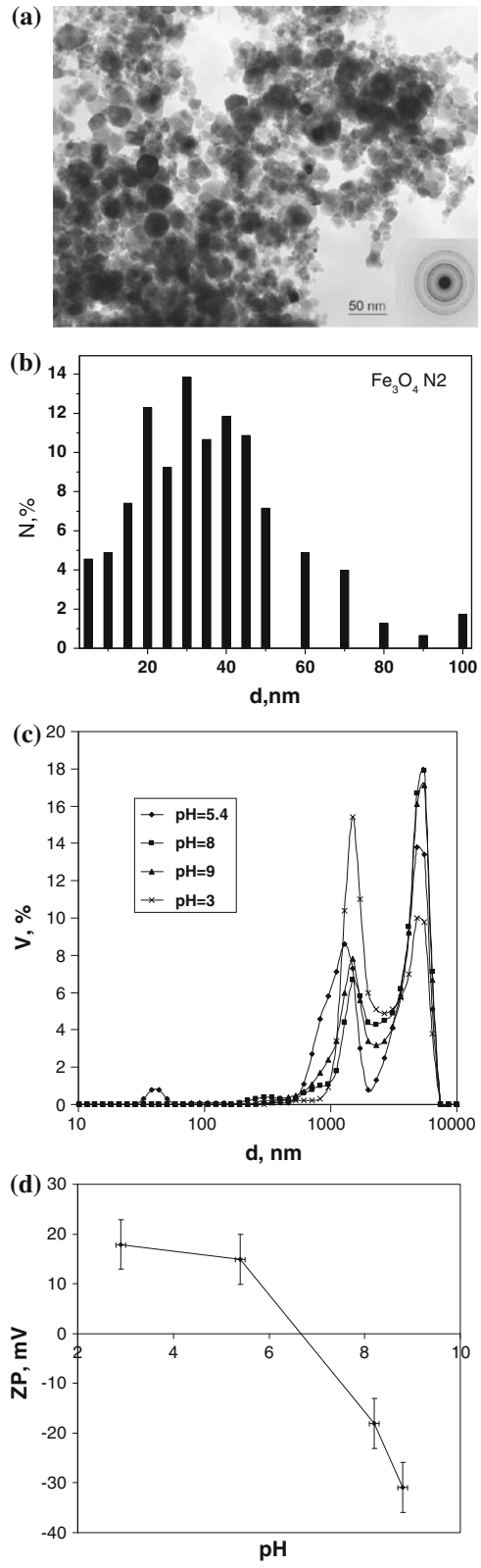

Fig. 1 Characterization of the magnetite nanoparticles. **a** TEM ► image of the nanopowder sample N2, **b** the size-distribution histogram for the nanopowders sample N2, **c** the size-distribution function $V(d)$ for nanopowder sample N4 in water obtained from DLS analysis for different pH values, and **d** zeta potential of the magnetite nanoparticle sample N4 as dependant from pH of water solution

magnetite. The secondary phase (α-Fe) content was not more then 6%. In some cases the X-ray data showed the oxygen defect structure $Fe_3O_{4-\delta}$, which can be assigned to the oxygen-deficient surface of the particles.

The transmission electron microscopy (TEM) images were taken in a high resolution 200 kV CM30 microscope. The TEM images showed that the powders consisted of the particles of an octahedral shape with diameters ranging in the interval of several nms to 100 nm. Figure 1a shows an example, the TEM image of the magnetite powder samples N2. From the TEM images the size-distribution histograms $N(d)$ for each powder were obtained (e.g., Fig. 1b). For every histogram, more then 1,000 particles were counted from the TEM microphotographs. To get the distribution function $N(d)$ in nanopowders is rather untrivial problem and different approaches are explored. Among these are the gas desorption Brunauer–Emmett–Teller (BET) method, magnetization analysis, dynamic light scattering by powder suspension, aggregation, and sedimentation analysis (Phenrat et al. 2007; Berret et al. 2007; Martinez-Pedrero et al. 2008; Goya et al. 2003).

The dynamic light scattering (DLS) measurements were performed using NanoZS apparatus (Malvern, UK). Laser beam $\lambda = 633$ nm was produced by He–Ne laser, operating in back-scattering mode at an angle of 173°.

In this study, the magnetite particle sizes in dry powders were estimated by three independent methods: (i) by direct measurements of the particle diameter from TEM pictures, (ii) from coherent scattering radius obtained from X-ray analysis, and (iii) from the specific surface data obtained by BET method. The second two methods are in a reasonable agreement with the particle size corresponding to the maximum of the $N(d)$ histograms.

The distribution functions $N(d)$ and $V(d)$ for the nanopowders in water were obtained from the photo-sedimentation method and from dynamic light scattering (DLS) (Fig. 1c). From the first method the

distribution functions $N(d)$ correspond to the main fractions of several micron sizes with a small part of nanosized particles. The DLS method gives the three-modal function $V(d)$ with one slight peak around d close to 50 nm, and two higher peaks with d close to 1 and 5 μm, correspondingly. The effect of pH on size-distribution functions is demonstrated in Fig. 1c. After the mixing the magnetite nanopowders with distilled water pH = 5.4 was measured. Both increase and decrease of pH from this value results in a redistribution of particles. For $2.9 < \text{pH} < 8.8$ investigated the measured ZP $\ll$ 30–40 mV (Fig. 1d), consequently, this corresponds to a region of the colloid instability of the suspension. The sedimentation dynamic was studied mainly at pH = 5.4 conditions.

The magnetization of nanopowders was measured at room temperature in magnetic fields up to 27 kOe using a vibrating sample magnetometer (Fig. 2a). At low temperatures (down to 2 K) and in magnetic fields up to 50 kOe a SQUID magnetometer was used (Fig. 2b). The magnetization curves show a saturation magnetization, which is an indication of the ordering of spontaneous magnetic moments. However, the saturation magnetization values at room and at low temperatures are about 10–20% lower than that in a bulk magnetite, which points to the presence of phases with lower magnetization. This might result from small nanoparticles ($d < 5$ nm) in the superparamagnetic state and/or the magnetically disordered shells of the particles. The complex magnetic structure of nanosized magnetite particles was confirmed by the shifted hysteresis loop (Fig. 2b). The shifted hysteresis loops have been often observed for small ferromagnetic particles and were explained by unidirectional anisotropy by coexistence of ferro- and antiferromagnetic interactions at the core/shell interface (Meiklejohn and Bean 1957; Ong et al. 2009; Iglesias et al. 2007). However, such an exchange bias was not observed in magnetite nanoparticles as prepared by chemical precipitation method (Goya et al. 2003), which confirms the strong dependence of the magnetic properties on the preparation method.

The presence of the surface oxygen deficiency in the magnetite nanopowders is confirmed by the Mossbauer spectra, which evidence a distribution Fe^{2+} and Fe^{3+} different from that in bulk natural magnetite Fe_3O_4. Figure 3 shows the Mossbauer spectrum for the Fe_3O_4 powder sample N2 and corresponding internal magnetic field distribution function $P(H)$. The spectrum

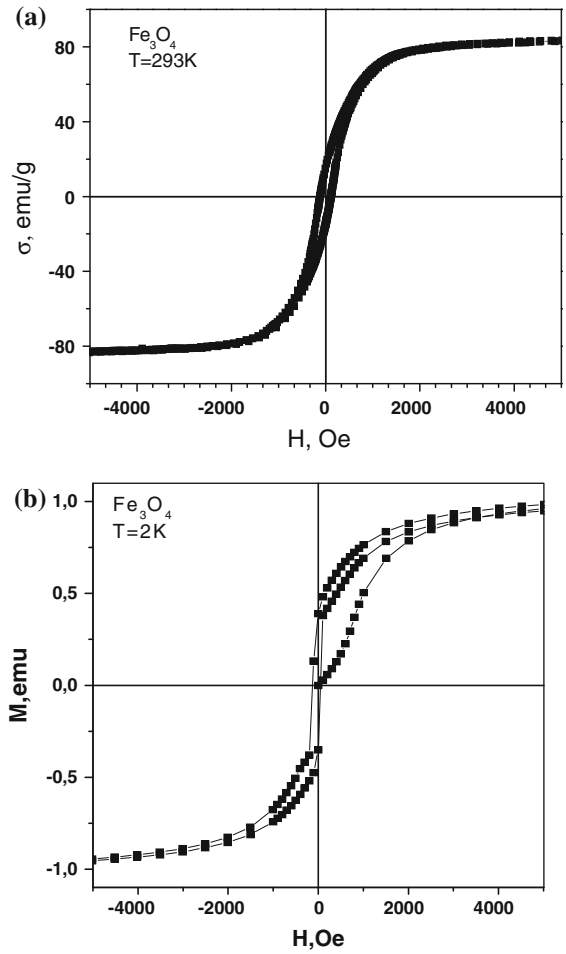

Fig. 2 Hysteresis loops of magnetite nanopowder sample N2 at room temperature and at low temperature

can be presented as a superposition of several partial spectra corresponding to a Fe^{3+} cations in tetragonal A-positions of spinel structure ($H = 492$ kOe), to Fe^{2+} and Fe^{3+} in octahedral B-positions (452 kOe), to zerovalent α-Fe ($\sim 5\%$) and to a doublet corresponding to a superparamagnetic phase of small magnetite particles (for this sample is about 5%). The maximum around $H = 427$ kOe might correspond to Fe-ions which are located in external surface layers with different defect surroundings.

Experimental

To study the sedimentation of magnetite nanoparticles in water the suspensions with different magnetite powder concentration (0.05–5 g/L) in distilled water

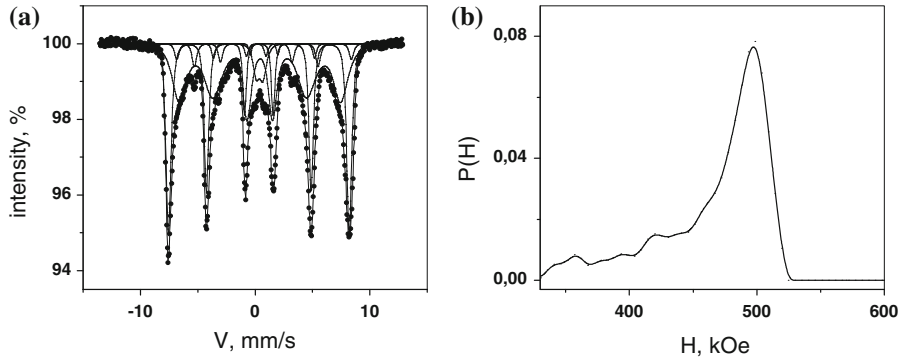

Fig. 3 Mossbauer spectrum (**a**) and corresponding internal magnetic field distribution function (**b**) for magnetite nanopowder sample N2

were prepared using ultrasonic treatment for about 10 s. As a rule for each sedimentation measurements a freshly made suspension was used. All the graphs presented refer to a magnetite powder concentration in water solution of 5 g/L.

The sedimentation was registered by monitoring the light transmission coefficient k. In optical set up a monochrome light beam with 950 nm wavelength in horizontal direction was split into two beams, one going through a pure water and another going through a fluid optical cell containing the magnetite suspension. Then the beams were detected by photodiodes and the ratio between the signals was amplified and PC-monitored versus time. Before each sedimentation experiment a calibration of the optic cell using pure transparent water was done. Under the optical cell with the magnetite suspension the magnetic systems can be placed.

The magnetic field source (magnetic system) was made from a set of six Sm_2Co_{17} permanent magnets with a coercive force $H_c = 16$ kOe and remanence induction Br = 10 kGs (Fig. 4a). The outer diameter

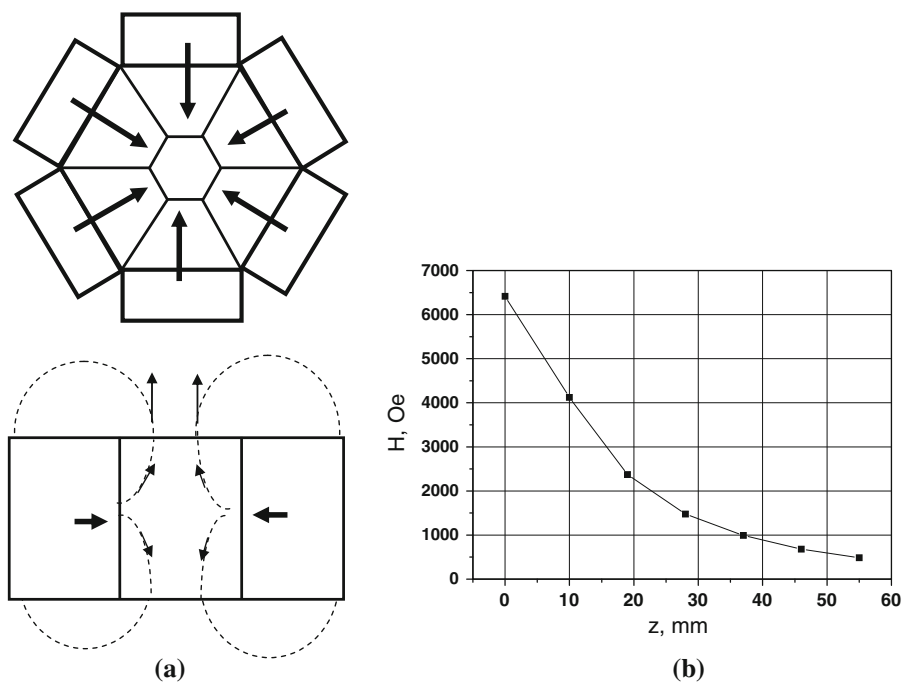

Fig. 4 Scheme of the permanent magnets system in horizontal plane (*above*) and a side view (*below*). The *bold arrows* show the magnetic field directions. The *dashed lines* and the *thin arrows* show the magnetic field distribution inside of the magnetic system where the fluid optical cell is placed (**a**). The distance dependence of the magnetic field along the vertical z-direction in the center of the magnetic system (**b**)

was 116 mm, the inner diameter was 18 mm, and the height was 40 mm. To enhance the magnetic field strength in internal space a soft magnetic steel road was inserted into the system channel. The value of the magnetic field and the gradient in vertical z-direction was measured using a Hall gauge. The magnetic field in the center of the optical cell was 6.4 kOe with a gradient of 1.6 kOe/cm (Fig. 4b).

Results and discussions

To illustrate the sorption capacity of the magnetite nanopowder as a prospective water cleaning agent Fig. 5 shows a sorption of Cr(VI) and Cu(II) from a model water solution by Fe_3O_4 nanopowders (20–50 nm). The sorption of Cr(VI) by magnetite nanoparticles can be significantly enhanced by heating of the water solution up to 50–60 °C (Linnikov et al. 2010). The process is irreversible, which might point to its chemisorption nature. These results are in agreement with the data obtained for the particles of about 10 nm as prepared by the sol–gel method (Hu et al. 2004). According to other researchers works in water solution for $0.9 \leq \text{pH} \leq 6.5$ the main chemical form of chromium is $HCrO_4^-$. (Buerge and Hug 1997; Venditti et al. 2010) and the main chemical form of copper is Cu^{2+} (Zhao et al. 2010). For the rest it is out of the scope of this study owing to the complicated chemistry.

Our study (Linnikov et al. 2010) had demonstrated that the Cr(VI) sorption by Fe_3O_4 nanoparticles was not different for any of the three preparation routes—chemical precipitation, gas-condensation, and laser evaporation methods. It has been shown that although the nanoparticles tend to aggregate into clusters of micron sizes this has no large effect on the sorption capacity of the powders. The coarse aggregates were very steady and were not significantly destroyed by ultrasonic agitation of the water solution, the aggregate sizes decreased from tens down to several microns. The Cr(VI) sorption experiments were performed both for the initial powder and for the powder after ultrasonic agitation, which showed practically the same results. Although rather complex chemistry is involved in dissolution of magnetite in water and in Cr(VI) and Cu(II) sorption processes (Buerge and Hug 1997) these results confirm the good perspectives to use magnetite nanopowders as a sorbents for these harmful elements removal from water.

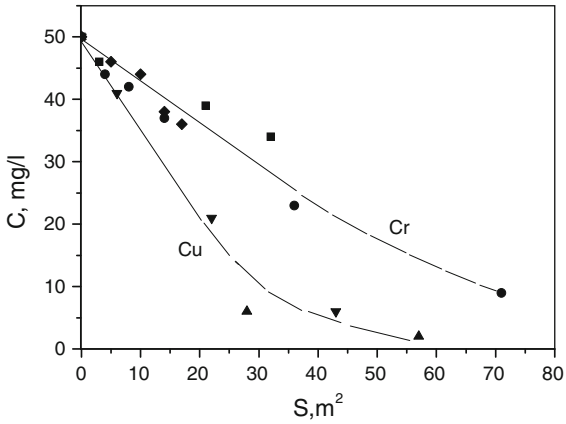

Fig. 5 Cr(VI) and Cu(II) metal cation concentrations versus the total surface area of the Fe_3O_4 nanopowder sorbent in a model water solution at $T = 290$ K (pH = 5.4)

Figure 6 shows the sedimentation dynamic curves for the nanopowder magnetite samples with different particle sizes. The fast change in k(t) corresponds to a faster particles sedimentation, and evidently a change in the sedimentation rate reflects a change in the particle mass due to the aggregation process. For the sample N2 the particles sediment rather fast—it requires about 500 s for a 90% sedimentation. A similar sedimentation was observed for the sample N4. The suspension with the samples N1 and N3 remain more stable for a long time. For example, for the sample N1 no sedimentation was observed during 1,500 min; after this time a fast sedimentation process appeared, resulting in 90% sedimentation (Fig. 6b).

The sedimentation process for both the large and small particles is of rather complex character, as it is illustrated in Fig. 6b, c. Larger particle start to sediment early, that is after several seconds (τ_1) with different speed, as it is marked in Fig. 6c. One could suggest that the characteristic times τ_1, τ_2, and τ_3 correspond to different stages of aggregates formation. The time up to τ_1 is needed for small particles to aggregate to larger clusters, which is accompanied by a slow sedimentation. Then for $\tau_3 > t > \tau_1$ the stage of intense sedimentation follows, where one could also observe some time interval with different sedimentation speed. And at $t > \tau_3$ the sedimentation goes very slowly as most of the heavy large aggregates have been already sedimented and only the smaller particles which have remained contribute to the change observed. For smaller particles the features of the

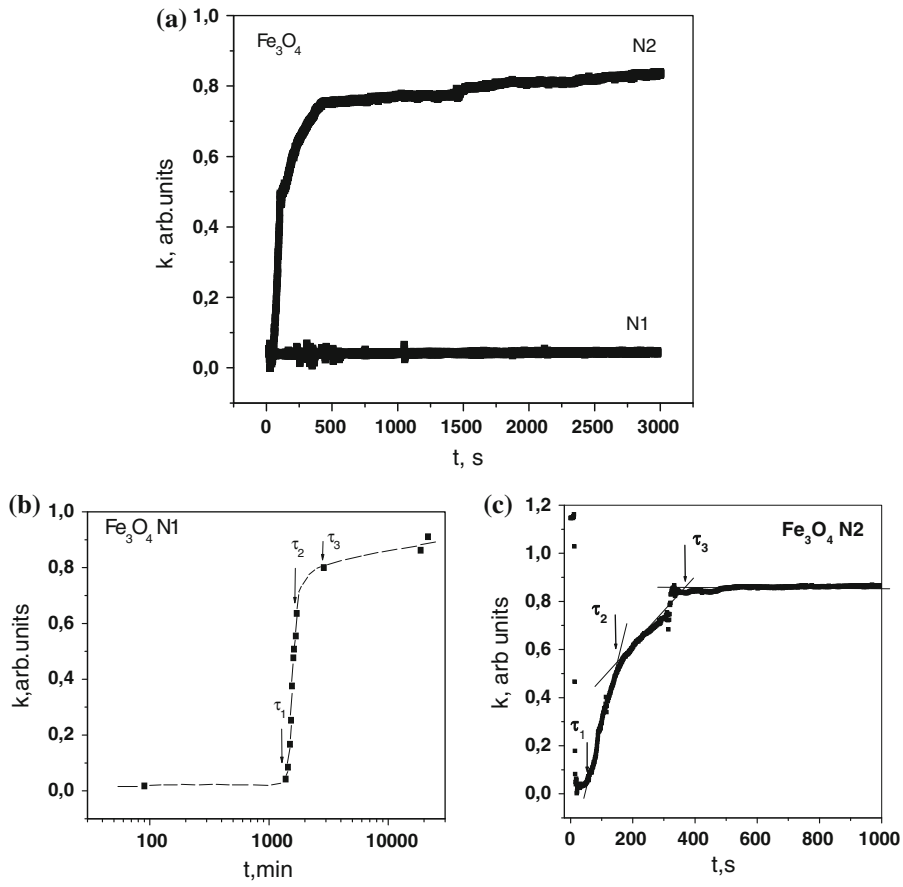

Fig. 6 **a** Time dependence of the monochrome light transmission coefficient k (sedimentation dynamic curve) for different Fe_3O_4 powder samples, **b**, **c** the specific features of the sedimentation dynamic curve for smaller (16 nm) and larger (54 nm) nanoparticles

sedimentation curves are similar, however, the characteristic aggregate formation time is much bigger—$\tau_1 = 11{,}000$ min, as it is shown in Fig. 6b.

The aggregates formation is also reflected in the sedimentation regimes observed for the freshly made Fe_3O_4 N1 suspension and for the same suspension prepared several weeks before (Fig. 7). Although qualitatively the sedimentation curves are similar, for freshly made suspension τ_1 is about 25 h, while for the old suspension $\tau_1 \sim 300$ s. In our previous study (Linnikov et al. 2010) a sedimentation analysis of the aggregates in long before prepared water suspensions has been done. The aggregates in several days old suspensions were of several tens microns sizes. The ultrasonic treatment could not fully destroy the big particle aggregates but could only reduce the average size down to several microns, so the time of intense sedimentation stayed of the order of the magnitude of several hundreds seconds. The qualitative difference between freshly made and old suspensions is a manifestation of the aging effects, which are important

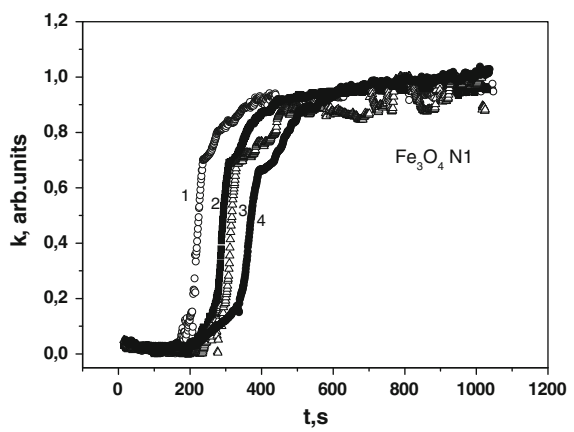

Fig. 7 Sedimentation dynamic curve for the "aged" magnetite nanopowder sample N1 in initial state (*1*) and after cycles of ultrasonic treatment (*2* → *4*)

for colloid stability in nanopowders (Tombácz et al. 2007).

Similar complex sedimentation curves were observed for the water suspension of iron and its

oxides in other study (Phenrat et al. 2007). By in situ optical observation of the zero-valent iron nanoparticles in water solution it had been shown that first small chains of particles are formed, then they aggregate into larger particles and at last a gelation of micrometer-size aggregates appears with almost close to zero sedimentation speed.

The sedimentation rate of magnetite nanoparticles in water solution is defined by the aggregates formation, which in turn in the framework of the DLVO theory depends on a competition between repulsive electrostatic forces and attractive van der Waals forces and attractive magnetic interaction forces acting between magnetite particles. These forces can be tuned by external factors, such as the particle concentration in the water solution, pH of the solution, and the external gradient magnetic field (Svoboda and Zofka 1983; Eberbeck et al. 2006).

The electrostatic force referred to the double layer of counter ions can be effectively changed by pH variation, which is a strong mean to regulate the colloid stability of suspensions. Also, one could suspect that both the electrostatic and magnetic interaction might be affected by existence of atomic and structural defects on the particle surface even when the chemistry involved (pH of the solution, ionic strength, etc.). In our experiments, the Fe_3O_4 nanoparticles obtained by different preparation techniques were studied (Linnikov et al. 2010), so they evidently had different defect states of the surface. However, the experiments did not show any remarkable difference in the aggregates formation and sorption process for these nanopowders. The interparticle magnetic interactions depend on the strong magnetization of the particles core, while a defect upper layer brings about some reduction of the total magnetization of the particles.

Figure 8 shows the effect of pH of the solution on the magnetite particles settling. The starting pH = 5.4 was measured just after the mixing the magnetite nanopowders with distilled water. One can see that the pH value variation in the range $2.9 \leq \text{pH} \leq 8.8$ makes a moderate effect on the sedimentation rates, while the sedimentation regime stays the same. So, both electrostatic and magnetic interactions are essential for the aggregates formation; their relative role needs to be clarified by further research.

The effect of external vertical gradient magnetic field on the Fe_3O_4 nanoparticles sedimentation is shown in Fig. 9a, b. The powder sample N4 with the

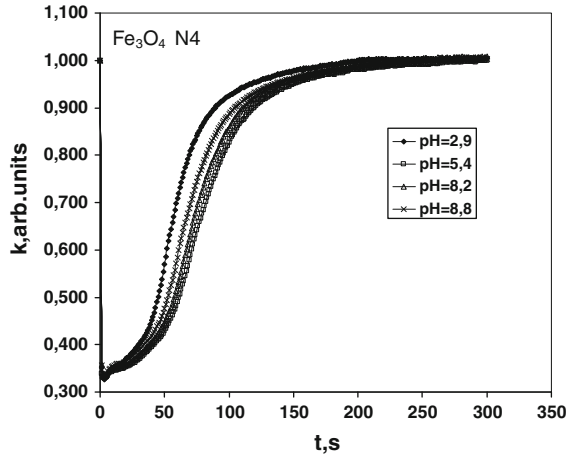

Fig. 8 Sedimentation dynamic curves for the magnetite nanopowder sample N4 at different pH

large particles starts to sediment after $\tau_1 \approx 50$ s in the absence of magnetic field, while under the action of the gradient magnetic field its 80% sedimentation is finishing within the first 20 s. In the next 200 s the full sedimentation is achieved (Fig. 9a). One can clearly see the characteristic times $\tau_2 \approx 20$ s and $\tau_3 \approx 100$ s with different sedimentation rates, which could evidence the fast particle aggregation in the magnetic field followed by a heavy aggregate sedimentation processes, as it was discussed earlier. The Fe_3O_4 powder sample N1 with the smaller particles shows good sedimentation already after 100 s in a gradient magnetic field, while it will require more then 24 h to sediment in the absence of magnetic field (Fig. 6b).

The data in the vertical gradient magnetic field evidence that not only a simple interaction of gradient magnetic field with magnetic moment of the nanoparticles is important for sedimentation, but also a particle magnetic interactions giving rise to a big magnetic aggregates formation, which, in turn, strongly enhances the sedimentation processes. Indirect indication of the magnetic aggregation of iron oxides is a slowing down of the filtration processes in heavy metals contaminated tap water (Barkatt et al. 2009).

The force acting on the magnetic particle in a magnetic gradient field $F_{\text{mag}} = \mu_0 V(M \text{ grad } H)$, where $V = 4\pi/3(d/2)^3$ is the volume of the particle, M—magnetization in a given magnetic field H, μ_0—permeability in vacuum. This force is opposite to the Brownian motion force $F_{\text{Br}} \approx k_B T/d$, where Boltzman's constant $k_B = 1.38 \cdot 10^{-23}$ J/K. Comparing these two main forces we can roughly estimate the

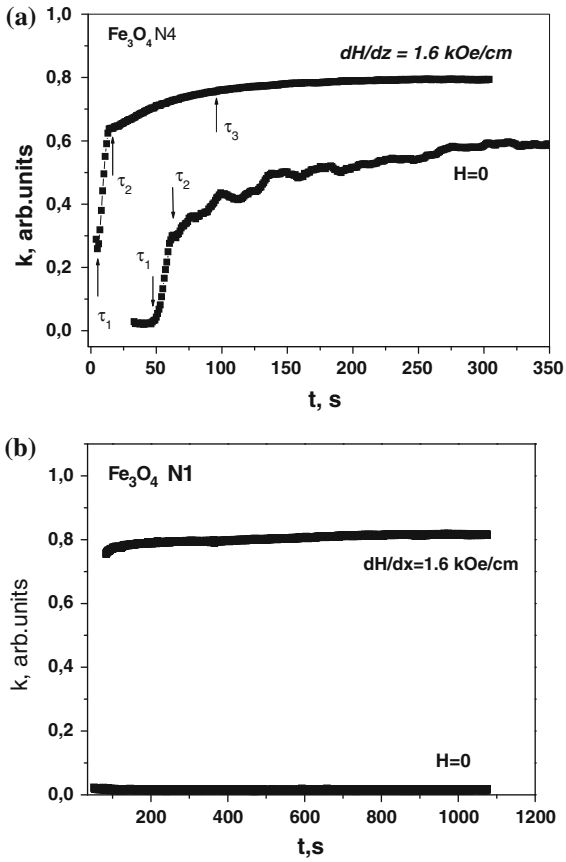

Fig. 9 The effect of the vertical gradient magnetic field on the sedimentation dynamic of the magnetite nanopowder samples N4 (**a**) and N1 (**b**) (pH = 5.4)

average size of the particles separated by the gradient magnetic field H before the aggregates formation. If we take the measured magnetization values at 300 K $\sigma_s \approx 70$ emu/g, the magnetic field gradient dH/d$z = 1.6$ kOe/cm we get $d \approx 100$ nm, which well exceed the size of the sedimenting particles in the powders investigated. Therefore, one can suggest that there are some additional contributions to magnetic interaction force. These might correspond to big magnetic aggregates and to additional magnetic field gradients on the particle surface.

The nanopowders prepared by most of contemporary methods present polydisperse mixtures of the particles with different sizes ranging from several nanometers to a hundreds nanometers. Among them are the particles which are in different magnetic states. If a particle size is below some critical value (for magnetite it is about 5 nm (Goya et al. 2003; Hsu et al. 2005), the particle is in a superparamagnetic state with low magnetic moment. Also there are ferromagnetic single-domain particles with high magnetic susceptibilities, and poly-domain ferromagnetic magnetic particles which have a lower magnetization in a magnetic field below saturation. The nanoparticles have a complex structure, where the outer layers have structural defects, local ionic disorder, oxygen deficiency etc., which is reflected in their magnetic structure and the resulting lower magnetization. One could speculate that the external magnetic field create an additional surface gradient, which enhances the interparticle magnetic interactions and promotes the particle aggregation (Yavuz et al. 2006), thus revealing a very useful feature related to the magnetite nanoparticles in a water solution.

The preparation of a monodisperse mixture of magnetite nanoparticles, as a rule requires an additional separation process. While it is approved for some biochemical applications, it will be rather costly for a ground water cleaning. So, one should consider more economically produced magnetic sorbents, where one will have to deal with a polydisperse powder. The effective removal of the magnetite sorbent from water solution will require a strong F_{mag}. To obtain a larger F_{mag} one must increase either the magnetic field gradient or the particle volume (V), which will, however, reduce a total surface of the powder. Hence, here one meets the optimization problem to achieve a high sorption capacity simultaneously with a good magnetic separation potential. The main variable parameters are: particles size distribution, average particle size, particle concentration in water suspension, pH of the water solution, magnetic field strength, and gradient which depends on the set up configuration of the permanent magnets.

From our results it follows that the optimal average magnetite particle size to remove metallic cations from water solution is around 50–80 nm. Even in the absence of an external magnetic field such nanoparticles effectively interact as magnetic dipoles, thus creating large and heavy aggregates which sediment within a reasonably short time (several minutes). To speed up the sedimentation of the smaller particles (of about 20 nm and less) an external magnetic field is very helpful. Using a gradient magnetic field system one can achieve a good sedimentation in water solution already after several minutes. To produce a high gradient magnetic field permanent magnets with

a high remanence and a corresponding configuration of the poles could be used. Such a magnetic system does not require electric energy and it is not degrading by corrosion, so the magnetic separation process looks inexpensive and rather promising for water cleaning techniques, in particular when removing heavy metals from waste and ground waters.

Conclusions

Magnetite nanopowders with the particles of the 20- to 80-nm average diameter are very promising as sorbents to remove metallic cations from polluted waters. It is shown that the use of magnetic field of 6 kOe with a vertical gradient of about 1.6 kOe/cm produced by a permanent magnets system will speed the sedimentation process up to several minutes. For a further recommendation for application in real cleaning water devices the optimization problem should be solved where the entering parameters are the particles size, pH of water solution, magnetic field strength, the gradient of magnetic field, the water layer depth, the water flow speed etc. The optimal permanent magnets configuration adjustment is under investigation.

Acknowledgments The study was supported from the grant N 12-I-2-2037 of the Ural Division of the Russian Academy of Sciences.

References

Barkatt A, Pulvirenti AL, Adel-Hadadi MA, Viragah C, Senftle FE, Thorpe AN, Grant JR (2009) Composition and particle size of superparamagnetic corrosion products in tap water. Water Res 43(13):3319–3325

Berret J-F, Sandre O, Mauger A (2007) Size distribution of superparamagnetic particles determined by magnetic sedimentation. Langmuir 23(6):2993–2999

Buerge IJ, Hug SJ (1997) Kinetics and pH dependence of chromium(VI) reduction by iron(II). Environ Sci Technol 31(5):1426–1432

Eberbeck D, Wiekhorst F, Steinhoff U, Trahms L (2006) Aggregation behaviour of magnetic nanoparticle suspensions investigated by magnetorelaxometry. J Phys Condens Matter 18:S2829–S2846

Goya GF, Berquo TS, Fonseca FC, Morales MP (2003) Static and dynamic magnetic properties of spherical magnetite nanoparticles. J Appl Phys 94(5):3520–3528

Hsu KH, Wu JH, Huang YY, Wang LY, Lee HY, Lin JG (2005) Critical size effects on the magnetic resonance in Fe_3O_4 nanoparticles. J Appl Phys 97:114322-1-4

Hu J, Lo IMC, Chen G (2004) Removal of Cr(VI) by magnetite nanoparticles. Water Sci Technol 50(12):139–146

Hu J, Chen G, Lo IMC (2005) Removal and recovery of Cr(VI) from wastewater by maghemite nanoparticles. Water Res 39(18):4528–4536

Iglesias O, Batlle X, Labarta A (2007) Modelling exchange bias in core/shell nanoparticles. J Phys Condens Matter 19: 406232–406236

Illes E, Tombacz E (2006) The effect of humic acid adsorption on pH-dependent surface charging and aggregation of magnetite nanoparticles. J Colloid Interface Sci 295(1): 115–123

Kortov VS, Ermakov AE, Zatsepin AF, Uimin MA, Nikiforov SV, Mysik AA, Gaviko VS (2008) Specific features of luminescence properties of nanostructured aluminum oxide. Phys Solid State 50(5):957–961

Linnikov OD, Medvedeva IV, Rodina IV, Uimin MA, Yermakov AYe, Platonov VV, Osipov VV, Shevchenko VG (2010) Removal of Cr(VI) from aqueous solutions by magnetite nanoparticles. Proceedings of the IWA conference, Moscow, No. 64

Liu JF, Zhao ZS, Jiang GB (2008) Coating Fe_3O_4 magnetic nanoparticles with humic acid for high efficient removal of heavy metals in water. Environ Sci Technol 42(18): 6949–6954

Martinez-Pedrero F, El-Harrak A, Fernandez-Toledano JC, Tirado-Miranda M, Baudry J, Schmitt A, Bibette J, Callejas-Fernandes J (2008) Kinetic study of coupled field-induced aggregation and sedimentation processes arising in magnetic fluids. Phys Rev B 78:011403-1-6

Meiklejohn WH, Bean CP (1957) New magnetic anisotropy. Phys Rev 105(3):904–913

Ong QK, Wei A, Lin XM (2009) Exchange bias in Fe/Fe_3O_4 core–shell magnetic nanoparticles mediated by frozen interfacial spins. Phys Rev B 80:134418-1-6

Phenrat T, Saleh N, Sirk K, Tilton RD, Lowry GV (2007) Aggregation and sedimentation of aqueous nanoscale zerovalent iron dispersions. Environ Sci Technol 41(1): 284–290

Svoboda J, Zofka J (1983) Magnetic flocculation in secondary minimum. J Colloid Interface Sci 94:37–44

Tartaj P, Morales MP, Veintemillas-Verdaguer S, Gonzáles-Carreno T, Serna CJ (2003) The preparation of magnetic nanoparticles for application in biomedicine. J Phys D 36(13):R182–R197

Tiwari DK, Behari J, Sen P (2008) Application of nanoparticles in waste water treatment. World Appl Sci J 3:417–433

Tombácz E, Illés E, Majzik A, Hajdú A, Rideg N, Szekeres M (2007) Ageing in the inorganic nanoworld: example of magnetite nanoparticles in aqueous medium. Croat Chem Acta 80:503–515

Tuutijärvi T, Lu J, Sillanpää M, Chen G (2009) As(V) adsorbtion on maghemite nanoparticles. J Hazard Mater 166(2–3): 1415–1420

Venditti F, Cuomo F, Ceglie A, Ambrosone L, Lopez F (2010) Effects of sulfate ions and slightly acidic pH conditions on Cr(VI) adsorption onto silica gelatin composite. J Hazard Mater 173:552–557

Yantasee W, Warner CL, Sangvanich T, Addleman RS, Wiacek RJ, Fryxell GE, Timchalk C, Warner MG (2007) Removal of heavy metals from aqueous systems with thiol

functionalized superparamagnetic nanoparticles. Environ Sci Technol 41(14):5114–5119

Yavuz CT, Mayo JT, Yu WW, Prakash A, Falkner JC, Yean S, Cong L, Shipley HJ, Kan A, Tomson M, Natelson D, Colvin V (2006) Low-field magnetic separation of monodisperse Fe_3O_4 nanocrystals. Science 314(10):964–967

Yuan P, Fan M, Yang D, He H, Liu D, Yuan A, Zhu J, Chen T (2009) Montmorillonite-supported magnetite nanoparticles for the removal of hexavalent chromium [Cr(VI)] from aqueous solutions. J Hazard Mater 166(2–3):821–829

Zhang W (2003) Nanoscale iron particles for environmental remediation. An overview. J Nanopart Res 5(3–4):323–332

Zhao G, Zhang H, Fan Q, Ren L, Chen Y, Wang X (2010) Sorption of copper(II) onto super-adsorbent of bentonite–polyacrylamide composites. J Hazard Mater 173:661–668

Zhong LC, Hu JS, Liang HP, Cao AM, Song WG, Wan LJ (2006) Self-assembled 3d-flowerlike iron oxide nanostructures and their application in water research. Adv Mater 18(18):2426–2431